JOC Featured Article

DFT Study on Bifunctional Chiral Brønsted Acid-Catalyzed Asymmetric Hydrophosphonylation of Imines

Masahiro Yamanaka* and Takashi Hirata

Department of Chemistry, Faculty of Science, Rikkyo University, 3-34-1 Nishi-Ikebukuro, Toshima-ku, Tokyo 171-8501 Japan

myamanaka@rikkyo.ac.jp

Received February 24, 2009

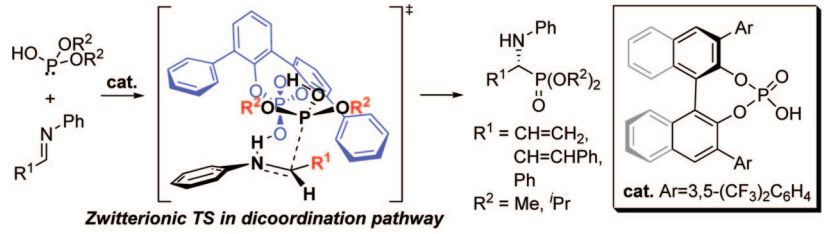

Asymmetric hydrophosphonylation reaction of aldimines with dialkyl phosphites proceeds catalytically by means of a phosphoric acid diester, derived from (*R*)-BINOL, as a chiral Brønsted acid to afford α-amino phosphonates with good to high enantioselectivities (up to 90% ee). The use of the aldimines derived from cinnamaldehyde derivatives and sterically demanding dialkyl phosphites was essential for achieving high enantioselectivity as well as high yield. To elucidate the reaction mechanism and the origin of the high enantioselectivity, DFT calculation (BHandHLYP/6-31G*) was carried out. The reaction proceeds via the nine-membered zwitterionic transition state (TS) with the chiral phosphoric acid, where aldimine and phosphite could be activated by the Brønsted acidic site and Lewis basic site, respectively. The *si*-facial attacking TS could be less favored by the steric repulsion of 3,3′-aryl groups on the chiral phosphoric acid with the bulky phosphite. When using the aldimine derived from benzaldehyde, the *re*-facial attacking TS is destabilized to decrease the enantioselectivity in agreement with the experimental results.

Introduction

Enantiomerically pure α-amino phosphoric acids and their phosphonate esters have attracted considerable attention in modern pharmaceutical chemistry because of their intriguing biological activities. As phosphorus analogues of α-amino acids, they have been employed as protease inhibitor,[1] antibacterial,[2] and anti-HIV[3] agents. Because biological activity depends on their absolute configuration at the α-carbon atom, catalytic enantioselective synthesis of α-amino phosphoric acid derivatives has been an important topic in organic chemistry. The most straightforward strategy to synthesize optically active α-amino phosphonic acid derivatives is based on enantioselective addition of an appropriate phosphorus nucleophile to imines. Therefore, considerable effort has been directed toward the development of the enantioselective catalytic hydrophosphonylation reaction over the past several years.[4] Several studies on the catalytic enantioselective hydrophosphonylation reaction of imines catalyzed by chiral metal catalysts have been reported.[5] In contrast, the organocatalytic versions have been scarcely investigated.[6−9] Asymmetric organocatalysis using a wide range of small molecules has recently emerged as an essential tool of

(1) Hirschmann, R.; Smith, A. B., III.; Taylor, C. M.; Benkovic, P. A.; Taylor, S. D.; Yager, K. M.; Sprengler, P. A.; Benkovic, S. J. *Science* **1994**, *265*, 234–237.

(2) (a) Allen, J. G.; Atherton, F. R.; Hall, M. J.; Hassall, C. H.; Holmes, S. W.; Lambert, R. W.; Nisbet, L. J.; Ringrose, P. S. *Nature (London)* **1978**, *272*, 56–58. (b) Atherton, F. R.; Hassall, C. H.; Lambert, R. W. *J. Med. Chem.* **1986**, *29*, 29–40. (c) Pratt, R. F. *Science* **1989**, *246*, 917–919.

(3) Alonso, E.; Solis, A.; del Pozo, C. *Synlett* **2000**, 698–700.

(4) For reviews on enantioselective catalytic hydrophosphonylation, see: (a) Groger, H.; Hammer, B. *Chem.—Eur. J.* **2000**, *6*, 943–948. (b) Merino, P.; Marqués-López, E.; Herrera, R. P. *Adv. Synth. Catal.* **2008**, *350*, 1195–1208.

(5) (a) Sasai, H.; Arai, S.; Tahara, Y.; Shibasaki, M. *J. Org. Chem.* **1995**, *60*, 6656–6657. (b) Gröger, H.; Saida, Y.; Arai, S.; Martens, J.; Sasai, H.; Shibasaki, M. *Tetrahedron Lett.* **1996**, *37*, 9291–9292. (c) Gröger, H.; Saida, Y.; Sasai, H.; Yamaguchi, K.; Martens, J.; Shibasaki, M. *J. Am. Chem. Soc.* **1998**, *120*, 3089–3103. (d) Saida, Y.; Gröger, H.; Maison, W.; Durot, N.; Sasai, H.; Shibasaki, M.; Martens, J. *J. Org. Chem.* **2000**, *65*, 4818–4825. (e) Kobayashi, S.; Kiyohara, H.; Nakamura, Y.; Matsubara, R. *J. Am. Chem. Soc.* **2004**, *126*, 6558–6559. (f) Saito, B.; Egami, H.; Katsuki, T. *J. Am. Chem. Soc.* **2007**, *129*, 1978–1986. (g) Abell, J. P.; Yamamoto, H. *J. Am. Chem. Soc.* **2008**, *130*, 10521–10523.

10.1021/jo900404b CCC: $40.75
Published on Web 04/02/2009

asymmetric organic synthesis. Jacobsen et al. reported that a chiral thiourea served as the efficient catalyst for the enantioselective hydrophosphonylation of *N*-benzylimines.[6] While high enantioselectivities were achieved for a wide range of both aliphatic and aromatic *N*-benzylimines, the highest selectivities were restricted to di(2-chloroethyl) phosphite and di(2-nitrobenzyl) phosphite. Petterson and Fini et al. also demonstrated a simple and efficient organocatalytic enantioselective hydrophosphonylation of imines.[7] By using commercially available quinine as the catalyst, the enantioselective addition of diethyl phosphite to *N*-Boc aromatic imines was achieved. In both cases, hydrogen bonding would exert a key role for electrophilic activation of imines. In particular, the DFT calculation elucidated that the thiourea catalyst activates the imine substrate by the dual hydrogen-bonding interaction of both urea hydrogens.[10]

In addition to chiral hydrogen-bonding catalysis, chiral Brønsted acid catalysis has become a vigorously growing trend in organocatalytic enantioselective reactions. The chiral phosphoric acid derived from an axially chiral substituent (e.g., BINOL) is, in particular, well-designed and conformationally rigid to transfer stereochemical information to the substrate through hydrogen-bonding network.[11,12] Recently, Akiyama and co-workers have demonstrated the chiral phosphoric acid derived from 3,3′-substituted (*R*)-BINOL **1** catalyzed asymmetric hydrophosphonylation reaction of *N*-arylimines (Scheme 1).[8] They proposed that Brønsted acidic (proton) and Lewis basic (phosphoryl oxygen) sites activate the imine substrate and the phosphorus nucleophile (e.g., phosphite),[13] respectively, to form

SCHEME 1. Asymmetric Hydrophosphonylation Reaction Catalyzed by the Chiral Phosphoric Acid

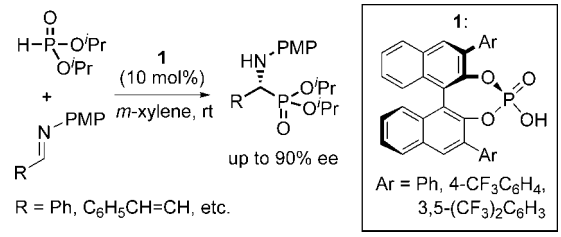

nine-membered cyclic transition state. The analogous chiral phosphoric acid catalyzed direct asymmetric Kabachnik−Fields reaction of aldehydes, anisidine, and di(3-pentyl)phosphite has been reported by List et al. most recently.[9] The chiral phosphoric acid bearing both Brønsted acidic and Lewis basic sites potentially allows for bifunctional catalysis to activate simultaneously both electrophile and nucleophile. Such a cooperative reaction mechanism via hydrogen-bonding interaction has emerged as an important paradigm of organocatalysis. However, it has been still unclear in most cases.[14] Herein, we reveal the reaction mechanism of the phosphoric acid catalyzed hydrophosponylation through understanding of the dual role of the phosphoric acid by DFT calculations. The origin of the enantioselectivity was also described in detail.

Chemical Model and Computational Method

In the asymmetric hydrophosphonylation reaction catalyzed by the chiral BINOL-derived phosphoric acid **1**, both reactivity and enantioselectivity were retarded using trialkyl phosphite.[8] This indicates that the OH moiety of dialkyl phosphite plays a significant role in achieving high yield and enantioselectivity. The dual function of phosphoric acid in the hydrophosphonylation reaction, therefore, has been proposed as follows: the phosphoric acid proton electrophilically activates aldimine and the phosphoryl oxygen atom accepts the OH proton of phosphite. Finally, bond recombination simultaneously gives the α-amino phosphonate product and regenerates the catalyst. To elucidate the bifunctionality of the phosphoric acid, two possible pathways (path 1, monocoordination pathway; path 2, dicoordination pathway) of the hydrophosphonylation reaction were compared (Scheme 2). In path 1, aldimine is activated through the proton, keeping phosphite coordination to oxygen atom on the same phosphoric acid moiety. In contrast to path 1, path 2 allows for the dual function of the phosphoric acid moiety, which activates aldimine and phosphite on the Brønsted acidic (proton) and Lewis basic sites (phosphoryl oxygen), respectively. The issue of the *re*-facial selectivity using **1** was also addressed on the basis of the well-defined transition structure. As is reported experimentally, aldimines derived from cinnamaldehyde derivatives and sterically demanding phosphites are needed to achieve high enantioselectivity. Focusing on these substituent effects in both aldimine and phosphite, we revealed the origin of the enantioselectivity in the present reaction. To reduce a computational cost, a chiral phosphoric acid bearing biphenol unit (Ar = Ph) was used instead of **1** as a chemical model. All

(6) Joly, G. D.; Jacobsen, E. N. *J. Am. Chem. Soc.* **2004**, *126*, 4102–4103.
(7) Pettersen, D.; Marcolini, M.; Bernardi, L.; Fini, F.; Herrera, R. P.; Sgarzani, V.; Ricci, A. *J. Org. Chem.* **2006**, *71*, 6269–6272.
(8) Akiyama, T.; Morita, H.; Itoh, J.; Fuchibe, K. *Org. Lett.* **2005**, *7*, 2583–2585.
(9) Cheng, X.; Goddard, R.; Buth, G.; List, B. *Angew. Chem., Int. Ed.* **2008**, *47*, 5079–5081.
(10) Vachal, P.; Jacobsen, E. N. *J. Am. Chem. Soc.* **2002**, *124*, 10012–10013.
(11) For reviews on chiral Brønsted acid catalysis, see: (a) Pihko, P. M. *Angew. Chem., Int. Ed.* **2004**, *43*, 2062–2064. (b) Taylor, M. S.; Jacobsen, E. N. *Angew. Chem., Int. Ed.* **2006**, *45*, 1520–1543. (c) Akiyama, T.; Itoh, J.; Fuchibe, K. *Adv. Synth. Catal.* **2006**, *348*, 999–1010. (d) Connon, S. J. *Angew. Chem., Int. Ed.* **2006**, *45*, 3909–3912. (e) Akiyama, T. *Chem. Rev.* **2007**, 5744–5758. (f) Terada, M. *Chem. Commun.* **2008**, *35*, 4097–4112.
(12) For selected recent examples, see: (a) Akiyama, T.; Itoh, J.; Yokota, K.; Fuchibe, K. *Angew. Chem., Int. Ed.* **2004**, *43*, 1566–1568. (b) Uraguchi, D.; Terada, M. *J. Am. Chem. Soc.* **2004**, *126*, 5356–5357. (c) Uraguchi, D.; Sorimachi, K.; Terada, M. *J. Am. Chem. Soc.* **2004**, *126*, 11804–11085. (d) Uraguchi, D.; Sorimachi, K.; Terada, M. *J. Am. Chem. Soc.* **2005**, *127*, 9360–9361. (e) Rowland, G. B.; Zhang, H.; Rowland, E. B.; Chennamadhavuni, S.; Wang, Y.; Antilla, J. C. *J. Am. Chem. Soc.* **2005**, *127*, 15696–15697. (f) Hoffmann, S.; Seayad, A. M.; List, B. *Angew. Chem., Int. Ed.* **2005**, *44*, 7424–7427. (g) Akiyama, T.; Morita, H.; Fuchibe, K. *J. Am. Chem. Soc.* **2006**, *128*, 13070–13071. (h) Akiyama, T.; Tamura, Y.; Itoh, J.; Morita, H.; Fuchibe, K. *Synlett* **2006**, 141–143. (i) Terada, M.; Machioka, K.; Sorimachi, K. *Angew. Chem., Int. Ed.* **2006**, *45*, 2254–2257. (j) Terada, M.; Sorimachi, K.; Uraguchi, D. *Synlett* **2006**, 133–136. (k) Storer, R. I.; Carrera, D. E.; Ni, Y.; MacMillan, D. W. C. *J. Am. Chem. Soc.* **2006**, *128*, 84–86. (l) Seayad, J.; Seayad, A. M.; List, B. *J. Am. Chem. Soc.* **2006**, *128*, 1086–1087. (m) Chen, X.-H.; Xu, X.-Y.; Liu, H.; Cun, L.-F.; Gong, L.-Z. *J. Am. Chem. Soc.* **2006**, *128*, 14802–14803. (n) Terada, M.; Sorimachi, K. *J. Am. Chem. Soc.* **2007**, *129*, 292–293. (o) Kang, Q.; Zhao, Z.-A.; You, S.-L. *J. Am. Chem. Soc.* **2007**, *129*, 1484–1485. (p) Guo, Q.-X.; Liu, H.; Guo, C.; Luo, S.-W.; Gu, Y.; Gong, L.-Z. *J. Am. Chem. Soc.* **2007**, *129*, 3790–3791. (q) Jia, Y.-X.; Zhong, J.; Zhu, S.-F.; Zhang, C.-M.; Zhou, Q.-L. *Angew. Chem., Int. Ed.* **2007**, *46*, 5565–5567. (r) Rueping, M.; Sugiono, E.; Schoepke, F. R. *Synlett* **2007**, 1441–1445. (s) Rueping, M.; Sugiono, E.; Theissmann, T.; Kuenkel, A.; Koeckritz, A.; Pews-Davtyan, A.; Nemati, N.; Beller, M. *Org. Lett.* **2007**, *9*, 1065–1068. (t) Rueping, M.; Theissmann, T.; Kuenkel, A.; Koenigs, R. M. *Angew. Chem., Int. Ed.* **2008**, *47*, 6798–6801. (u) Terada, M.; Tanaka, H.; Sorimachi, K. *Synlett* **2008**, 1661–1664. (v) Itoh, J.; Fuchibe, K.; Akiyama, T. *Angew. Chem., Int. Ed.* **2008**, *47*, 4016–4018. (w) Itoh, J.; Fuchibe, K.; Akiyama, T. *Synthesis* **2008**, 1319–1322. (x) Akiyama, T.; Honma, Y.; Itoh, J.; Fuchibe, K. *Adv. Synth. Catal.* **2008**, *350*, 399–402.
(13) The phosphite tautomer has a lone pair at the phosphorus atom to undergo nucleophilic addition. It is known that the phosphorus nucleophile reacts as the active phosphite form generated via phosphonate−phosphite tautomerization. See ref 5d.
(14) For theoretical studies on the chiral phosphoric acid catalysis, see: (a) Yamanaka, M.; Itoh, J.; Fuchibe, K.; Akiyama, T. *J. Am. Chem. Soc.* **2007**, *129*, 6756–6764. (b) Simón, L.; Goodman, J. M. *J. Am. Chem. Soc.* **2008**, *130*, 8741–8747. (c) Marcelli, T.; Hammar, P.; Himo, F. *Chem.−Eur. J.* **2008**, *14*, 8562–8571. (d) Simón, L.; Goodman, J. M. *J. Am. Chem. Soc.* **2009**, *131*, 4070–4077.

SCHEME 2. Mechanism of the Hydrophosphonylation Reaction Catalyzed by the Chiral Phosphoric Acid

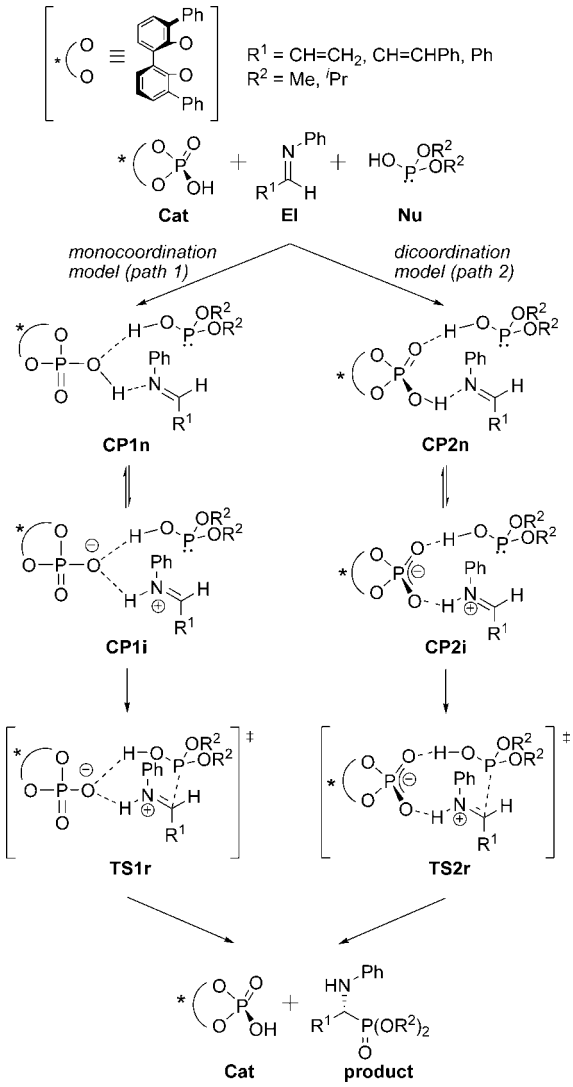

calculations were performed with the Gaussian 98 package.[15] Geometries were fully optimized and characterized by frequency calculation using hybrid density functional theory (BHandHLYP)[16] with the 6-31G*.[17] Free energies were also computed for the gas phase. Natural charges from the natural population analysis were calculated at the same level as the one used for the geometry optimization.

Results and Discussion

Two pathways (path 1, monocoordination pathway; path 2, dicoordination pathway) in the case of R^1 = vinyl and R^2 = Me were first explored. In both paths 1 and 2, there are two possible models of aldimine activation: protonation and hydrogen-bonding models. Protonation of aldimine generates a zwitterionic complex of iminium salt (**CP1i** or **CP2i**) followed by nucleophilic attack of dialkyl phosphite (**Nu**). In activation by hydrogen bonding, proton abstraction proceeds after the C−P bond formation directly from **CP1n** or **CP2n**. We explored the transition state (**TS**) of the C−C bond formation for two activation models. As a result, zwitterionic transition structures (**TS1r** and **TS2r**) were only found. The present hydrophosphonylation reaction, therefore, would proceed predominantly through protonation followed by nucleophilic attack via zwitterionic **TS** as in the Mannich-type reaction catalyzed by a similar phosphoric acid.[14a]

We compared the relative energies of hydrogen-bonding complexes (**CPn**), zwitterionic complexes (**CPi**), and transition states (**TS**) on paths 1 and 2 (Figure 1). All stationary points in path 2 are more stable than those in path 1, and hence, path 2 is the thermodynamically favorable route. The zwitterionic complexes (**CP1i** and **CP2i**), generated by protonation, are more stable than the hydrogen-bonding complexes (**CP1n** and **CP2n**)

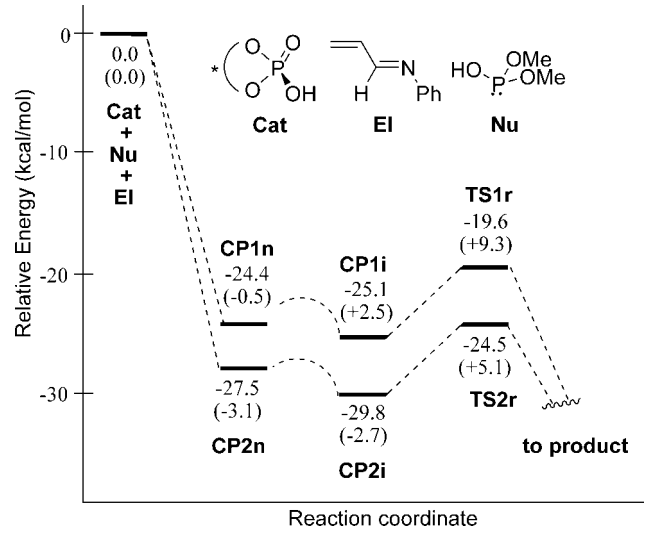

FIGURE 1. Energy profiles (R^1 = CH=CH_2, R^2 = Me) of monocoordination pathway (path 1) and dicoordination pathway (path 2). The potential energy of the sum of Cat, Nu, and El is set to zero. The free energies are shown in parentheses.

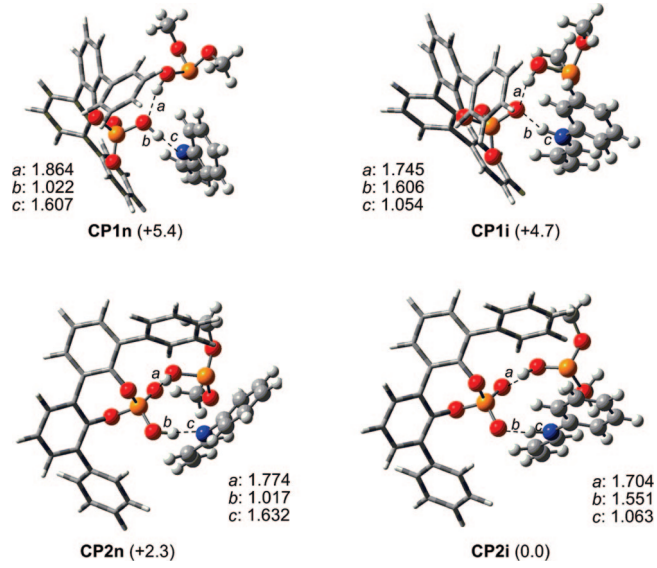

FIGURE 2. 3D structures of **CP1n**, **CP1i**, **CP2n**, and **CP2i** at the BHandHLYP/6-31G* level. Bond lengths are in Å. Relative energies (kcal/mol) are shown in parentheses.

(15) Gaussian 98, Revision A.11.4. Frisch, M. J. et. al. Gaussian, Inc.: Pittsburgh, PA, 2002.

(16) The default Gaussian 98 implementation of the BHandHLYP method does not correspond to the original definition by Becke. For the original version, see: Becke, A. D. *J. Chem. Phys.* **1993**, *98*, 1372–1377.

(17) Hehre, W. J.; Radom, L.; Schleyer, P. v. R.; Pople, J. A. *Ab initio Molecular Orbital Theorey*; John Wiley: New York, 1986, and references cited therein.

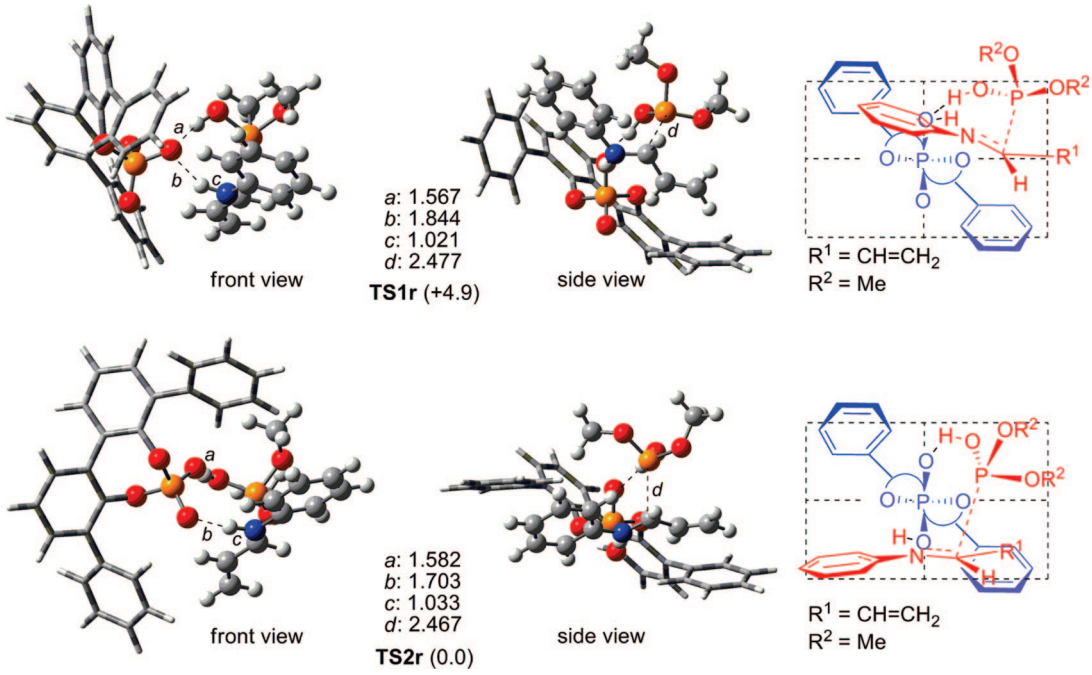

FIGURE 3. 3D structures and schematic representation models of **TS1r** and **TS2r** at the BHandHLYP/6-31G* level. Bond lengths are in Å. Relative energies (kcal/mol) are shown in parentheses.

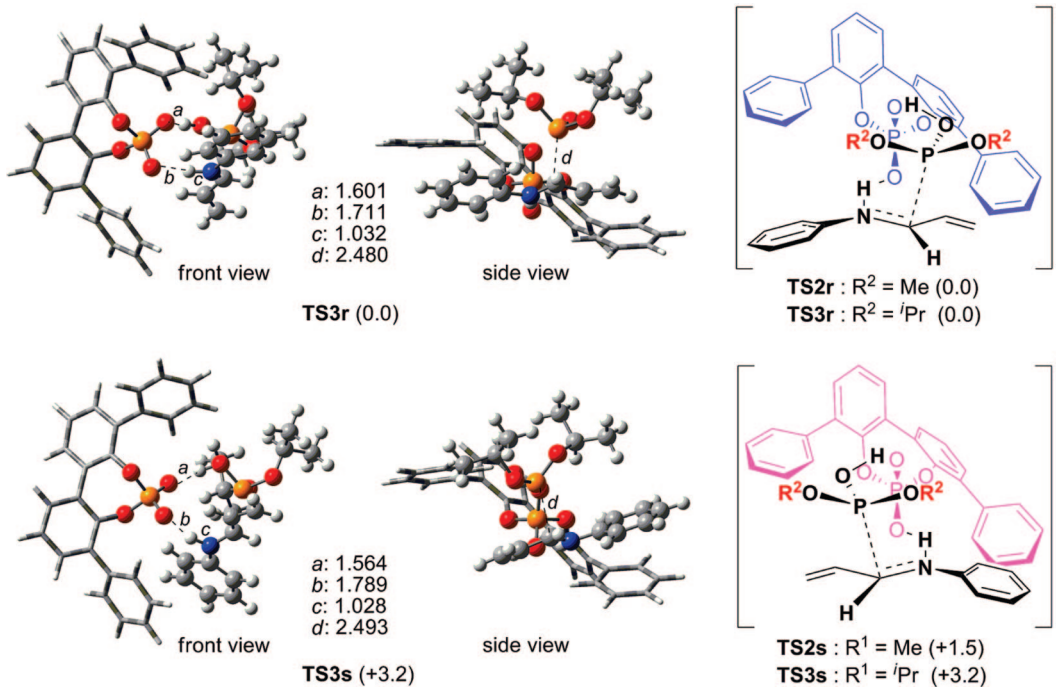

FIGURE 4. 3D structures and schematic representation models of **TS3r** and **TS3s** at the BHandHLYP/6-31G* level. Bond lengths are in Å. Relative energies (kcal/mol) are shown in parentheses.

by only ca. 2 kcal/mol in energy. The proton-transfer reaction, therefore, would exhibit a very flat energy profile to be ignored in this study.[18] In both path 1 and path 2, nucleophilic attack of dimethyl phosphite via zwitterionic **TS** exhibited moderate activation barriers, ca. 5 kcal/mol (ca. 7 kcal/mol in free energy). The seven-membered cyclic **TS1r** is found to be higher in energy than the nine-membered cyclic **TS2r** by 4.9 kcal/mol (4.2 kcal/mol in free energy). Thermodynamic stabilization of dicoordination model (path 2) through the whole reaction pathway is achieved by the dual function of the phosphoric acid moiety.

Figures 2 and 3 show the 3D pictures of important stationary points. Comparison of 3D pictures indicates that **CPn** and **CPi** have almost the same gross structures other than the hydrogen-bonding moiety (Figure 2). The lengths of O−H (*a*, *b*) and N−H (*c*) are changed dramatically through protonation. Almost the same two P−O bonds (1.501, 1.482 Å) are only observed in **CP2i**, where the negative charge is delocalized over the O−P−O

(18) This is very similar with the phosphoric acid catalyzed Mannich-type reaction; see ref 14a.

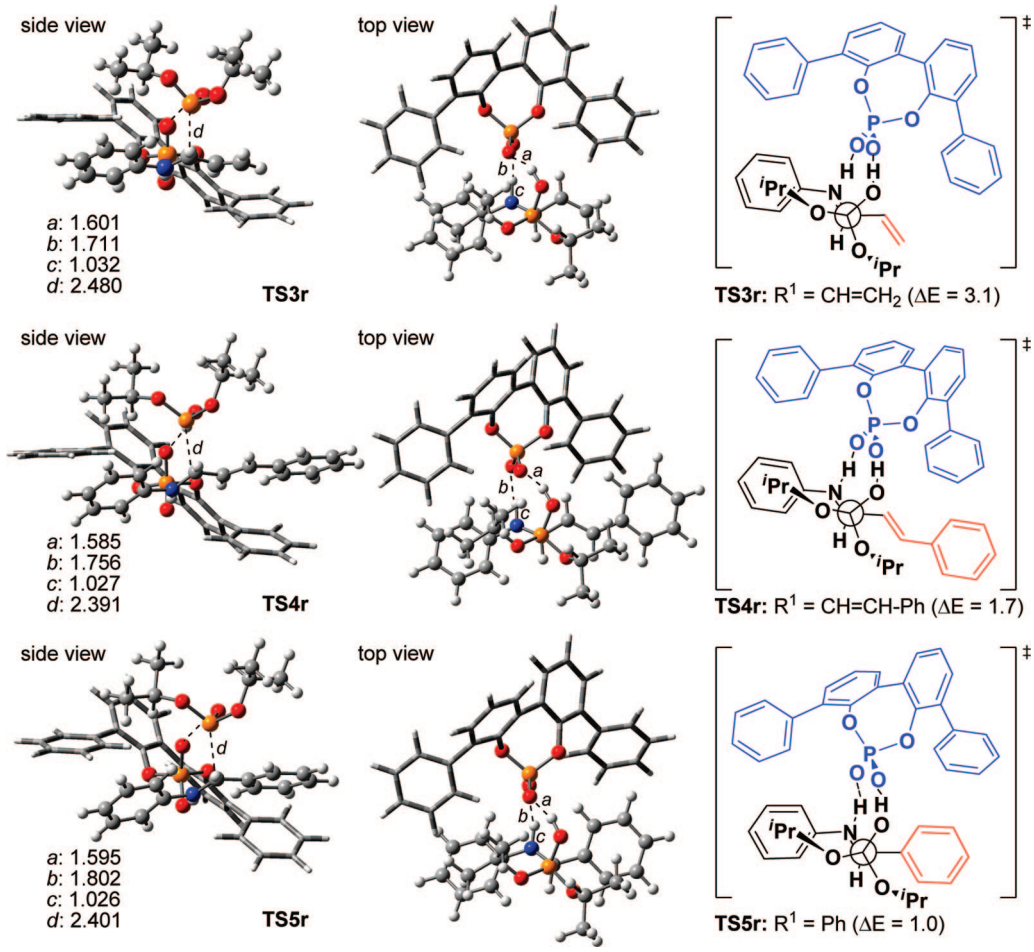

FIGURE 5. 3D structures and schematic representation models of **TS3r** and **TS3s** at the BHandHLYP/6-31G* level. Bond lengths are in Å. Energy differences $\Delta E = E(\mathbf{TSs}) - E(\mathbf{TSr})$ (kcal/mol) are shown in parentheses.

fragment trapping phosphite and iminium. Two P−O bonds in other complexes are regarded as the P═O double bond (ca. 1.47 Å) and the P−O single bond (ca. 1.51−1.55 Å). While Lewis basic phosphoryl oxygen coordinates to the phosphite OH group in **CP2**, both phosphite and iminium (or imine) coordinate to the single-bonded terminal oxygen atom (or the OH moiety) in **CP1**. The lengths of *a*, *b*, and *c* are comparable to thermodynamic stability of **CP2**, which has the stronger hydrogen-bonding interaction among phosphite, iminium (or imine), and the phosphoric acid moiety than **CP1**. In particular, **CP2i** is stabilized by the resonance stabilization on the O−P−O fragment in combination with the hydrogen-bonding interaction between substrates and the phosphoric acid catalyst.

The transition structures on path 1 and path 2 are illustrated in Figure 3. While the relative location between substrates and the phosphoric acid catalyst is retained, the hydrogen-bonding network around the phosphoric acid moiety is critically changed. In both **TS1r** and **TS2r**, the lengths between the phosphoryl oxygen atom and phosphite (O−H; *a*) are shortened in comparison to the corresponding **CPi**s (**CP1i**: 1.745 Å, **TS1r**: 1.567 Å, **CP2i**: 1.704 Å, **TS2r**: 1.582 Å). On the other hand, the lengths between the phosphoryl oxygen atom and iminium (O−H; *b*) are lengthened (**CP1i**: 1.606 Å, **TS1r**: 1.844 Å, **CP2i**: 1.551 Å, **TS2r**: 1.703 Å). At the stage of C−P bond formation, the phosphoryl oxygen atom accepts the OH proton of phosphite, and consequently the hydrogen-bonding interaction between the phosphate anion moiety and iminium is weakened. The steric hindrance in C_2-symmetric (*R*)-3,3′-Ph_2-BINOL-derived phosphoric acid is concentrated in the upper left-hand and lower right-hand quadrants (side views in Figure 3). In **TS1r**, both iminium and phosphite are located at the empty upper right-hand quadrant due to their coordination with one phosphoryl oxygen atom. As a result, both substrates (red in the schematic representation of **TS1r**) are directed away from the bulky 3,3′-positioned phenyl groups, which is responsible for asymmetric induction. This indicates that the facial selectivity of nucleophilic addition to iminium could not be controlled in **TS1r**. In sharp contrast, the energetically favored **TS2r** results from placing the bulky substituents of iminium and phosphite in the empty site of the phosphoric acid catalyst. In **TS2r**, each of two phosphate oxygen atoms binds with iminium and phosphite leaving sterically demanding groups (*N*-phenyl and R^2 groups in the schematic representation of **TS2r**) toward the empty lower left-hand and upper right-hand quadrants. Such a two-point binding nine-membered cyclic TS model of **TS2r** is expected to yield the facial selectivity of nucleophilic addition. This result motivated us to elucidate the origin of the enantioselectivity through exploring the substituent effects of imine (R^1) and phosphite (R^2).

It was experimentally exhibited that the higher enantioselectivity was obtained by using $(^i\mathrm{PrO})_2$POH rather than $(\mathrm{MeO})_2$POH. Screening of imine substrates showed aldimines derived from cinnamaldehyde derivatives are essential for the high enantioselectivity. Focusing on the substituent effect of phosphite, comparison of the transition state corresponding to the favored *re*-facial attacking TS (**TSr**) with the *si*-facial

attacking TS (**TSs**) was first studied in both cases of R^2 = Me (**TS2**) and ^{i}Pr (**TS3**) (Figures 4). Both the *re*-facial attacking **TS2r** and **TS3r** are energetically more favored than the *si*-facial attacking **TS2s** and **TS3s**. The energy difference between the two diasteromeric transition states, **TS3r** and **TS3s**, is larger than that between **TS2r** and **TS2s**. This indicates that more bulky phosphite (e.g., R^2 = ^{i}Pr) could yield the higher enantioselectivity in agreement with the experimental result. In contrast to the *re*-facial attacking phosphite, *si*-facial attacking phosphite is located at the sterically demanding upper left-hand quadrant to lead to steric repulsive interaction. Therefore, **TS3s** is more destabilized in comparison to **TS2s** because of the greater steric repulsion between the 3,3′-positioned phenyl group and phosphite. The similar transition-state model has been shown in Goodman's recent DFT study on the chiral phosphoric acid catalyzed Strecker reaction.[14d] The enantioselectivity of this reaction has been explained by the steric interaction between the phosphoric acid and the imines. In contrast, our transition-state model indicates the steric interactions of the phosphoric acid with the bulky groups of phosphite would be major factors in the energy difference of the diastereomeric transition states.

To investigate the R^1 substituent effect of aldimine for the enantioselectivity, three transition state models (R^1 = vinyl, styryl, phenyl) were explored (Figure 5). The energy difference (ΔE) between **TSr** and **TSs** increases with the decrease in the steric hindrance of R^1 in the following order; R^1 = phenyl (**TS5**) < styryl (**TS4**) < vinyl (**TS3**). This indicates that the styryl or vinyl substituent at R^1 of aldimine leads to the higher enantioselectivity than the phenyl substituent in agreement with the experimental result. In any transition state models, the energetically favored **TSr** results from placing R^1 substituent in the hindered lower right-hand quadrant, and hence **TS5r** having more bulky phenyl substituent produces the greater steric repulsion between the 3,3′-positioned phenyl group and R^1 than **TS4r** or **TS3r**. It is noted that destabilization of **TS5r** decreases the energy difference between **TSr** and **TSs** to result in the lower enantioselectivity.

Conclusion

DFT studies on the chiral phosphoric acid catalyzed asymmetric hydrophosphonylation reaction of aldimine and dialkyl phosphite were carried out. The chiral phosphoric acid plays a significant role for activation of both substrates. Lewis basic phosphoryl oxygen nucleophilically activates phosphite in combination with Bronsted acid activation of aldimine. Therefore, the C−P bond formation proceeds through the two-point binding nine-membered cyclic TS. The enantioselectivity would be originated from the relative stability of the two diastereomeric transition states. The *si*-facial attacking TS (**TSs**) is destabilized by the steric repulsion between the 3,3′-positioned phenyl group and phosphite substituent R^2 to enhance the enantioselectivity. On the other hand, the *re*-facial attacking TS (**TSr**) is destabilized to decrease the enantioselectivity as increasing the steric repulsion between the 3,3′-positioned phenyl group and aldimine substituent R^1.

Acknowledgment. We thank Prof. T. Akiyama for helpful discussions. Computational time from the Research Center for Computational Science, Okazaki, Japan is deeply acknowledged.

Supporting Information Available: Computational details (Cartesian coordinates and absolute energies for stationary points). This material is available free of charge via the Internet at http://pubs.acs.org.

JO900404B